ATMOSPHERIC OPTICS GROUP
Technical Note No. 263

Version 1.1
April 2004

Development of Techniques for Determination of Nighttime Atmospheric Transmittance and Related Analytic Support for the Whole Sky Imager

UNIVERSITY OF CALIFORNIA SAN DIEGO

SCRIPPS INSTITUTION OF OCEANOGRAPHY

Janet E. Shields
Art R. Burden
Monette E. Karr
Richard W. Johnson
Justin G. Baker

MARINE PHYSICAL LAB San Diego, CA 92152-6400

Development of Techniques for Determination of Nighttime Atmospheric Transmittance and Related Analytic Support for the Whole Sky Imager

Table of Contents

List of Illustrations

Tables

Development of Techniques for Determination of Nighttime Atmospheric Transmittance and Related Analytic Support for the Whole Sky Imager

Janet E. Shields, Art R. Burden, Monette E. Karr, Richard W. Johnson, and Justin G. Baker

1. Introduction

This report describes the work done for the Air Force Research Lab, Kirtland Air Force Base under Contract N00014-01-D-043 DO #5, between 24 May 01 and 17 Oct 03. The primary goal of this work was the development of techniques for extracting the atmospheric transmittance distribution over the sky, from Whole Sky Imager nighttime data.

2. Background

The Atmospheric Optics Group at the Marine Physical Lab, Scripps Institution of Oceanography, University of California San Diego, has been developing Whole Sky Imagers (WSI) for many years. (Johnson 1989, 1991). A Day/Night WSI which had 24-hour a day capability was initially developed in the early 1990's, and has been significantly upgraded in capability since that time (Shields 1993, 1998). One of these instruments, Day/Night WSI Unit 5, was delivered to the Air Force Research Lab, Kirtland Air Force Base, in December 95 for fielding at a remote site. The WSI was delivered to the sponsor under Contract N00014-93-D-0141 DO #11 (Shields, 1997a). (At that time, AFRL was named Phillips Laboratory, PL/LIO.) The instrument was operated under the sponsor's care at their site. The sponsor told us that the instrument "is an excellent source of data and is a very reliable system." Under follow-on contracts, several developments to software and documentation took place (Shields, 1997b and Shields, 2002).

Most recently, under funding from another sponsor, we evaluated and tested techniques for identifying the presence of clouds in the starlight images. This starlight cloud detection was based on the detection of stars in the image. Using the National Space Science Data Center catalog of stars, the algorithm predicts the location of the stars in the image, and attempts to detect each star. The point-spread function of the star is represented by a Gaussian of width of approximately 0.5 pixels. If the algorithm is able to detect this spatial signature at the appropriate location in the image, then the point is identified as cloud free.

Approximately 2100 stars per image are evaluated to form a cloud decision in approximately 237 regions (or cells) of the sky. Under subsequent funding from this other sponsor, this algorithm was further refined (including increasing the number of cells to 356), and converted to C code for processing efficiency.

Under funding from various sponsors, we had also developed techniques for providing radiometric calibration of the WSI images. Essentially, each pixel is calibrated to provide the radiance of the sky in the units of watt/Ω m^2 μm. The typical signal to noise for the darkest part of the sky between stars is typically about 40, providing very high quality raw data for calibration into the desired radiometric units.

By combining the techniques for star detection, and the techniques for absolute calibration, we developed, under this contract, new techniques for determination of optical beam transmittance of the atmosphere and semi-transparent clouds. Using a technique similar to the Gaussian fit used in the star detection, it is possible to integrate the area under the Gaussian, and relate this integrated signal to the star intensity. With an appropriate library of inherent star intensity, determination of the earth-to-space beam transmittance of the atmosphere and the semi-transparent clouds becomes possible.

3. Statement of Work

The Statement of Work from the proposal is as follows for the primary task:

The contractor shall, unless otherwise specified herein, supply the necessary personnel, facilities, services, and materials to accomplish the following tasks within a one-year period following receipt of funding.

1. Develop a library of star irradiances for use by the transmittance algorithm.

2. Provide radiometric calibration of the sensor, contingent on the sponsor delivering the sensor to MPL.

3. Evaluate techniques for determining earth-to-space beam transmittance distribution from WSI starlight imagery. Within the limits of funding, work toward development of these techniques in software code, which can be fielded with the AFRL WSI.

4. Provide a final written report and interim verbal reports to the sponsor regarding the results of the above work.

5. Other work such as minor repairs to the instrument are permissible under this task, if they are mutually agreed upon by the sponsor and by MPL to be appropriate. In this case, the work toward the other requirements in this statement of work would be lessened accordingly.

The primary task was fully funded (at $50,499), and in addition, a small increment of the optional task was funded (for $14,501). The optional task was:

1. Coordinate with the sponsor regarding the most appropriate tasks and estimated costs for development.

2. Provide personnel trained in the Whole Sky Imager and its capabilities to address these tasks (at MPL) to the limit of funding provided under the contract. These tasks may include analysis, software development, documentation, minor hardware development, and other tasks related to the WSI that are mutually agreed upon by the sponsor and by MPL to be appropriate.

3. Provide a final written report and interim verbal reports to the sponsor regarding the results of the above work.

This additional funding was intended to supplement the development and programming of the transmittance work.

All of the work was completed successfully, as will be discussed in the next sections.

4. Derivation of Star Irradiance Library and Equations for Extracting Beam Transmittance

In order to determine the beam transmittance, a primary input is the irradiance of a star in the absence of the atmosphere – which we will call the inherent irradiance of the star. In the following sections, we will define and derive an equation for determining the spectral irradiance of a star from known quantities. We will show how this can be used to determine the effective spectral irradiance of a star over our sensor's wavebands. Then we will derive the equation for the beam transmittance, and finally discuss how to use the radiances measured by our system in the derivation of the beam transmittance.

4.1. Spectral Irradiance of a Star - Definition

We start with the basic blackbody equation (Budding, 1993), which gives the spectral radiant emittance of a star.

$$W_\lambda = \frac{2\pi\ hc^2\ \lambda^{-5}}{\exp(hc/\lambda k\ Tc) - 1} \qquad \text{Eq. 1}$$

In this Blackbody equation (or Planck's equation), the terms are:

h = Planck's Constant = $6.626\ 10^{-34}$ J sec
c = speed of light = $2.998\ 10^{8}$ m sec^{-1}
λ = wavelength in m
k = Boltzmann's constant = $1.381\ 10^{-23}$ J K^{-1}
Tc = Color Temperature of the star in degrees K

If the star is a perfect blackbody, the color temperature is equal to its physical temperature. If the star is not a perfect blackbody, the color temperature is the temperature for which the blackbody equation most closely predicts the actual emittance.

Physically, spectral emittance is the energy, in Watts per unit surface area per unit wavelength, emitted by the star. In this case the surface involved is the surface of the star. In radiometrics, this would commonly be given in the units of $Watt/m^2\mu m$. In Equation 1, the units of the constants yield an emittance in J/sec m^3, which is equivalent to Watt/m^3. Thus if we want to convert the computed value to more standard radiometric units, we must multiply the result of Eq. 1 by $10^{-6}\ m/\mu m$.

Our sensor is calibrated to yield the absolute spectral radiance of an extended source. Spectral radiance is defined as the energy received per solid angle, per surface area, and

per wavelength, by a surface in a given direction. We usually use the units of $\mathrm{Watt/Sr\ m^2 \mu m}$

All stars except the sun form effectively a point source, when sensed by the WSI. That is, the surface area as seen from the earth by the WSI subtends less than a pixel. This means that the radiance is undefined. For now, in this derivation we will therefore derive the spectral irradiance of a star, rather than the spectral radiance, and deal with the conversion of our signals to irradiance later in this memo.

Irradiance is defined as the energy received per unit area on a surface. Similarly, spectral irradiance is the irradiance per wavelength. In this case, the surface involved is the surface of the earth, or more specifically, the effective surface of the sensor. The irradiance can be defined with respect to a horizontal surface, or a surface normal to the star. For this derivation, we will use a surface normal to the star. This will be mentioned again in Section V.

To derive the spectral irradiance E_λ created on a surface at a distance r by a star of spectral emittance W_λ and radius R, we first recognize that the star is spherical, and its surface is essentially Lambertian, meaning that its radiance is independent of viewing angle (Boyd, 1983). In a Lambertian source, it can be shown that the emittance W is related to the radiance L by

$$W = \pi L \qquad \text{Eq. 2}$$

(Eq. 2.22 in the above reference). Further, the total flux emitted by the sphere of radius R is given by Eq. 2.28 from the above,

$$\phi = 4\pi^2 R^2 L \qquad \text{Eq. 3}$$

The irradiance on a surface at distance r is given by Eq. 2.29,

$$E = \pi R^2 L/r^2 \qquad \text{Eq. 4}$$

Combining Eq. 4 with Eq. 2, we see that the irradiance may be derived from the emittance of a star by

$$E = R^2 W/r^2 \qquad \text{Eq. 5}$$

and the spectral irradiance may similarly be derived from the spectral emittance by

$$E_\lambda = R^2 W_\lambda /r^2 \qquad \text{Eq. 6}$$

Unfortunately, Eq. 6 is not of much use to us unless we know the distance and radius of a large set of stars. One of the references given to us by our sponsors in fact used this method (Riker, 1993) both to calibrate the sensor and to determine the beam transmittance to a few stars. (We have a very significant advantage over this method:

our sensor is small enough to be brought into a calibration room and be calibrated directly. This significantly lowers the uncertainty in the calibration.) We could use Eq. 6 to determine the irradiance of a star, however our sponsors told us they do not have large star libraries containing the star radius information. Therefore, we used an alternative approach based in part on Riker 1997, which utilizes libraries of visual star magnitude, which is documented for most of the stars in the standard star library we are using.

4.2. Using Visual Star Magnitude to Derive Visual Star Irradiance

The relative stellar magnitude is defined in a variety of ways. Budding defines it as

$$m1 - m2 = -2.5 \log(f_1/f_2) \qquad \text{Eq. 7}$$

where m1 and m2 are the magnitude of two stars, and f1 and f2 are defined as their flux. Flux is generally defined radiometrically as energy. Budding goes on to say that the above is too imprecise for scientific use, and therefore standard magnitude is defined using either V, B, or U, where V is the standard visual magnitude – a term he leaves undefined. We believe the V refers to power of the source integrated over the visual response curve. (B is Bolometric magnitude, which refers to the total power of the source integrated over all wavelengths, and U is ultraviolet.) So far we know that stellar magnitude refers to relative changes in energy from the star, such that a factor of 10 change in energy corresponds to a change of 2.5 in magnitude. This results from the historical relationship that a change of 5 in magnitude corresponded to a factor of 100 change in energy.

Riker (1997) states that Eq. 7 refers to brightness. However, he also uses Eq. 7 to define the relative change in visual irradiance, which he defines as

$$E_v = \int V(\lambda)\, E_\lambda \, d\lambda \qquad \text{Eq. 8}$$

Riker does not appear to define $V(\lambda)$ or list its values. However, Allen (1972) defines m_v as the apparent magnitude in the visual system as defined by the $V(\lambda)$ curve, which he lists in Section 97. This curve is similar to the Photopic and Scotopic response curves, which are the human visual response for day and night respectively, however, he states that the $V(\lambda)$ curve includes aluminum reflectivity (but not atmospheric absorption). The $V(\lambda)$, Photopic, and Scotopic response are shown in Table 1.

Riker then adds that the definition of a zero-magnitude source for visual magnitudes is

$$E_v(0) = 3.1623\ 10^{-9}\ \ \text{Watt}/\text{m}^2 \qquad \text{Eq. 9}$$

Combining Eq. 9 and 7, we have the visual irradiance for a star of magnitude m is given by

$$E_v(m) = E_v(0)\ 10^{-m/2.5} \qquad \text{Eq. 10}$$

Table 1
The V_λ Response in comparison with Photopic and Scotopic

λ(nm)	V_λ	Photopic	Scotopic
400	0.00	0.00	0.02
420	0.00	0.00	0.08
440	0.00	0.02	0.21
460	0.00	0.06	0.41
480	0.01	0.14	0.65
500	0.36	0.32	0.90
520	0.91	0.71	0.96
540	0.98	0.95	0.68
560	0.80	1.00	0.35
580	0.59	0.87	0.14
600	0.39	0.63	0.05
620	0.22	0.38	0.02
640	0.09	0.18	0.01
660	0.03	0.06	0.00
680	0.01	0.02	0.00

Our star library includes visual magnitudes of the stars for nearly all the stars. Thus we should be able to determine the visual irradiance of the star, or the spectral irradiance of the star integrated over the V_λ curve.

There is some uncertainty in the value for the visual irradiance for a zero-magnitude source. Riker lists his sources as Allen (1976) and Ramsey (1962). Ramsey lists the value as 3.1, rather than 3.1623. He says he uses the "visible response curve (standard observer)". This may be the Photopic curve than the V_λ curve given by Allen. We have not been able to find the source of Riker's number in the Allen reference. Also, Riker derives that the irradiance corresponding to the peak of the visual response curve is .0355 $W/m^2\mu m$. However, he states that others have obtained the values of .0380 and .0372. Lena (1988) lists the value as .0392, and Zombeck (1990) gives .0364. These values range to about 10% higher than the value given by Riker. The average value, .0373, is about 5% higher than Riker's value, indicating that a value closer to 3.32 10^{-9} may be more appropriate in Eq. 9. We used Riker's value, because this is the one our sponsors have historically used, so we should benefit from their experience with this issue.

4.3. Deriving Spectral Irradiance for the WSI Passbands

Because our sensor does not acquire information with a V_λ wavelength response, the information on the visual irradiance of a star is not yet sufficient. We need to know the effective spectral irradiance for our passbands. This is defined by

$$E(m) = \frac{\int E_\lambda(m)\ \overline{S_\lambda T_\lambda} d\lambda}{\int \overline{S_\lambda T_\lambda}\ d\lambda} \qquad \text{Eq. 11}$$

where E(m) is the irradiance for star magnitude m, in a given spectral filter and neutral density filter setting, and $\overline{S_\lambda T_\lambda}$ is the standard response in a given SP and ND filter.

Normally S_λ is the responsivity of the sensor, and T_λ is the product of the transmittance of all filters which are in place in a given SP and ND filter combination setting. The calibration for all of our instruments are adjusted to provide the radiances for an instrument of standard response, as defined in in-house Memo AV01-001t, and these responses are designated by $\overline{S_\lambda T_\lambda}$ as noted above. We will normally be working in the open hole configuration (Spectral 2, ND 1). Unless other specific designation is given, the equations that follow will be assumed to apply to the open hole. By use of a different $\overline{S_\lambda T_\lambda}$ curve, however, these equations can be applied to any of our other filter combinations.

To derive the value in Eq. 11, we need to derive a general equation for E_λ. Combining Eq. 8 and 6, we have

$$E_v(m) = \int E_\lambda \; V(\lambda) \; d\lambda = \frac{R^2}{r^2} \int \; W_\lambda V(\lambda) \; d\lambda = C \; \int W_\lambda \; V(\lambda) \; d\lambda \qquad \text{Eq. 12}$$

where C is a constant relating E_λ and W_λ as shown in Eq. 6 and defined below.

$$E_\lambda = CW_\lambda \qquad \text{Eq. 13}$$

From Eq. 12 and 10, we have

$$C = \frac{E_v(0) \; 10^{-m/2.5}}{\int W_\lambda \; V(\lambda) \; d\lambda} \qquad \text{Eq. 14}$$

Thus, in order to derive spectral irradiance for the WSI open-hole band, we use the defining equation 11, using the standard curves as input. The E_λ comes from Eq. 13, where C is defined in Eq. 14, and W_λ is defined in Eq. 1 (with the proper unit conversions).

Use of Eq. 1 requires knowledge of the color temperature of the star. The star library includes the "spectral types on the Morgan-Keenan (MK) classification system". The color temperature is roughly correlated with the spectral class, although there is some disagreement over the specific effective (or color) temperatures that correspond to each class. Table 2 shows values from Riker, Allen, and Zombeck. Riker provides a fairly complete list, but lists his source as "Davin, D., private communication". Allen often lists several temperatures for a given class. Where there are 3 temperatures for one class, the first in the table is for the "Main sequence, V", the second is for the "Giants, III", and the third is for "Super giants, I". That is, his temperature values depend not only on the spectral class but on a size class. Similarly, Zombeck lists values for the main sequence, and a second set of values (given in parenthesis) for giants. We chose to use a spectral

class table with 133 classifications from the Jet Propulsion Lab, as will be discussed in Section 6.

Clearly, there is a significant uncertainty in the derivation of the inherent irradiance from information available in the star library. This may be our largest source of uncertainty. However, if we use the existing information currently used by the sponsor, we should still see a very significant increase in the extent and accuracy of the beam transmittance values, for two reasons. First, because we are able to calibrate the WSI directly, we should have a much more accurate measurement of apparent irradiance as sensed at the earth surface. This should result in much more accurate transmittance estimates than was previously possible. Secondly, we can sense many stars simultaneously, and provide a distribution of transmittance estimates over the sky in place of a single estimate, thus providing a much more extensive amount of information. We will still be subject to the uncertainties in the inherent irradiance, but those uncertainties will at least be no worse than they are currently.

In the future, it seems very reasonable to use the WSI to evaluate how much the inherent irradiances should be changed. For example, by studying images taken throughout several clear, reasonably stable nights, we should be able to identify stars that yield consistently low or high results, and potentially adjust the inherent star irradiance library. In fact, if accurate knowledge of the inherent star irradiances becomes more critical, the possibility exists of using the WSI for a more detailed study. By using a photopic filter, along with the red and blue filters, and taking more extensive measurements from high altitude, it may be feasible to significantly improve the inherent star irradiance library for use with other applications. In the meantime, for this project, we used the values presented by Riker.

4.4. Definition of Earth-to-Space Beam Transmittance

Up until this point, the various irradiance values have all been for out of the atmosphere, i.e. with no atmospheric losses. As noted earlier, this is called the inherent irradiance. We will use the annotation E_0 to represent these inherent irradiances. As will be discussed in Section V, we will also be determining a measured irradiance, which is the irradiance from the ground. This includes the atmospheric transmission losses, and is known as the apparent irradiance. We will designate it E_A where A represents Apparent. (We would use M for Measured, however this could add confusion, since the star magnitude is m.)

In McCartney's text, he treats beam transmittance as a function of spectral irradiance. He states that a beam of spectral irradiance E_λ in going through a lamina of thickness x is attenuated according to

$$\frac{d\ E_\lambda}{E_\lambda} = \beta\ dx \qquad \text{Eq. 15}$$

where β is defined as the total scattering coefficient.

Table 2
Effective or Color Temperature vs. Star Class

Class	Tc Riker	Tc Allen	Tc Zombeck	Class	Tc Riker	Tc Allen	Tc Zombeck
A0	11000	9900, 12000	10800	G4	5578		
A1	10587			G5	5477	5520, 5000,4850	5610(5010)
A2	10189		9730	G6	5378		
A3	9806			G7	5281		
A4	9438			G8	5186		5490(4870)
A5	9083	8500	8620	G9	5092		
A6	8742			K0	5000	4900, 4500,4100	5240(4720)
A7	8413		8190	K1	4825		(4580)
A8	8097			K2	4656		4780(4460)
A9	7793			K3	4493		(4210)
B0	25000	28000, 30000	30000	K4	4335		(4010)
B1	23030		24200	K5	4183	4130, 3800,3500	(3780)
B2	21214		22100	K6	4037		
B3	19542		18800	K7	3895		4410
B4	18002			K8	3759		
B5	16583	15500	16400	K9	3627		
B6	15276		15400	M0	3500	3480,3200	3920(3660)
B7	14072		14500	M1	3407		3680(3600)
B8	12963		13400	M2	3317		3500(3500)
B9	11941		12400	M3	3229		3360(3300)
F0	7500	7400, 7000	7240	M4	3143		3200(3100)
F1	7335			M5	3060	2800	3120(2950)
F2	7173		6930	M6	2900		(2800)
F3	7014			O0	40000		
F4	6860			O1	38163		
F5	6708	6580	6540	O2	36411		
F6	6560			O3	34740		
F7	6415			O4	33145		
F8	6274		6200	O5	31623	40000	38000
F9	6135			O6	30171		38000
G0	6000	6030,5600, 5700	5920	O7	28786		38000
G1	5892			O8	27464		35000
G2	5785		5780	O9	26203		35000
G3	5681						

From this equation, we have the irradiance E_2 at distance x given by

$$E_2 = E_1 \exp(-\beta x) \qquad \text{Eq. 16}$$

where E_1 is the initial irradiance. Here the λ designation has been dropped, but it should be understood that these are still spectral quantities.

McCartney then defines transmittance, which we will designate by T, as

$$T = \frac{E_2}{E_1} = \exp(-\beta x) \qquad \text{Eq. 17}$$

The earth-to-space beam transmittance is the transmittance over a path from the earth surface to outside the earth atmosphere. Thus the transmittance is a ratio of the inherent spectral irradiance above the atmosphere E_λ to the apparent spectral irradiance at the earth surface E_A. In our case, we will be determining the effective transmittance over our passband, since we will be using the effective spectral irradiance of the star over our passband. Thus the equation for beam transmittance becomes

$$T = \frac{E_A}{E_0} \qquad \text{Eq. 18}$$

Whereas McCartney defines the beam transmittance in terms of the irradiance, Duntley (1975) defines the beam transmittance in terms of radiance, as in the following equation

$$L_r = L_o \;\; T_r + L_r^* \qquad \text{Eq. 19}$$

In this equation, L_r is the apparent radiance at the end of a path of length r, L_0 is the inherent radiance at the 0 point, Tr is the beam transmittance over the path, and Lr* is the path radiance due to light scattered into the path. This is the transmittance we are far more familiar with. If we remove the path radiance (as will be discussed in the next section), this is similar in form to Eq. 17. For our geometry, the distance between the star and a position on the earth's surface is nearly the same as the distance between the star and a position above the earth's atmosphere. As seen in Eq. 4, this means that over the distances we are dealing with, the change in irradiance due to the range change is insignificant. As a result, the change in irradiance which is due to the atmosphere is proportional to the change in radiance due to the atmosphere. This means that the beam transmittance defined in terms of irradiance is equivalent to the beam transmittance defined in terms of radiance, for this specific geometry, and using stars as the source. This is shown in Eq. 20.

$$\frac{L_r}{L_o} \approx \frac{E_r}{E_o} \equiv \frac{E_A}{E_0} = T \qquad \text{Eq. 20}$$

Note that in general the definition of beam transmittance based on irradiance may not be equivalent to the definition of beam transmittance based on radiance. However, as shown above, for the specific case of a star, the transmittances are equal. Had this not been the case, we would have needed to find out what type of transmittance our sponsors need to

know. Since we are using stars for our sources, the transmittance we determine using the irradiances will apply equally well to radiances as shown in Equation 20.

4.5. The Measured Apparent Irradiance of the Star

The WSI was designed to handle extended sources such as the sky, and it is calibrated to yield the spectral radiance defined by

$$L = \frac{\int L_\lambda \ \overline{S_\lambda T_\lambda} \ d\lambda}{\int \overline{S_\lambda T_\lambda} \ d\lambda} \qquad \text{Eq. 21}$$

where L is the total energy per solid angle and per unit surface area falling on a surface from a given direction.

For a single pixel, the irradiance produced on a horizontal surface by the radiance in the solid angle of the pixel is given by

$$E = \int \int L(\theta,\phi) \ \cos\theta \ d\Omega \qquad \text{Eq. 22}$$

Our sensor reports the actual radiance in the direction of a pixel, not the radiance modified by the cos term. In a sense, it shows the radiance falling on a surface normal to the direction sensed by the pixel. We will be evaluating the irradiance from a star. For the inherent star irradiance, We have used the irradiance on a plane normal to the star, rather than a horizontal plane. Since we are wishing to determine the irradiance on a plane normal to the star for a single pixel or a few pixels, then the irradiance equation for a single pixel reduces to

$$E = \int \int L(\theta,\phi) d\Omega = L \ \Delta\Omega \qquad \text{Eq. 23}$$

where L is the measured radiance, and $\Delta\Omega$ is the solid angle of the pixel.

Due to the slight defocusing of the optics and atmospheric turbulence the light from a star is not collected by a single pixel, but is distributed over a few pixels. The typical light distribution is approximately that of a Gaussian curve with a STD of approximately 0.5 pixel. The width of the Gaussian is reasonably constant over the image, but may vary from system to system depending on how well focused the sensor is.

If there were only one star in a given image, it would be a simple process to multiply the measured radiance in each pixel by that pixel's solid angle, and add the results. This works because the pixels on the CCD are contiguous, so no flux falls between pixels. In our images, with many stars, it may be possible to use a similar technique, perhaps adding the weighted signals over a 4 x 4 array of pixels with no other stars within the array. This is problematic in a crowded star field, so it may or may not be practical.

A second approach is to use the area under the Gaussian. Our current night cloud algorithm program does this with uncalibrated signals. We would need to apply

radiometric calibrations, to yield a radiance image, and then multiply each pixel by its solid angle, to yield irradiance for the pixel. Then the Gaussian algorithm could determine the area under the curve for each star. This approach has the advantage that the Gaussian best-fit technique already recognizes and removes nearby stars.

In both approaches outlined above, it is also necessary to subtract the background radiance that is scattered into the field of view by the sky. This is the Lr* term in Eq. 19. If we use the approach based on the Gaussian curve fit, this is already handled, because the program determines the background level and subtracts this from the star signal. If we use the approach of adding the signal from pixels near a star, we will similarly need to determine the background level for the region of the star, and subtract it.

4.6. Summary of Theoretical Derivation

The approach we used to estimate earth-to-space beam transmittance depends on knowing the inherent irradiance of a star above the atmosphere and determining the apparent irradiance of the star at the surface from the calibrated measurements of the WSI. The beam transmittance in the direction of that star can be determined from these values, and the variation in beam transmittance over the sky can be determined from using as many stars as is reasonable.

The inherent irradiance of a star on a surface normal to the star may be computed as described in Section 4.3. That is, we use the star spectral type from the catalog to determine color temperature, use Eq. 1 (with unit changes) to determine the emittance, use Eq. 13 to determine spectral irradiance, and use Eq. 11 to determine the spectral irradiance for the WSI passband. In Eq. 13, the constant C is determined from the visual magnitude of the star given in the star library using Eq. 14 and 9. These steps could be done once, to create a star spectral irradiance library to go with the star library.

The apparent irradiance of a star as measured by the WSI would be determined basically by subtracting the background radiance, multiplying each measured radiance by the solid angle of the pixel, and then combining the signals from those pixels affected by the star. Section V discusses this approach in more detail.

When the inherent irradiance E_0 and the apparent irradiance E_A are known, the earth-to-space beam transmittance is computed from Eq. 20. Note that in a clear atmosphere, the vertical beam transmittance $T(\theta = 0)$ is typically about 0.70 in the photopic (a rule of thumb from past experience), and the beam transmittance in the direction of a star should vary roughly by

$$T(\theta) = T(0)^{\sec\theta} \qquad \text{Eq. 24}$$

We will be determining the T value for each star, and so we should expect that on a clear night these values will decrease toward the horizon. In other words, our sponsors told us not to correct for the sec θ term, but rather to report the actual estimated transmittance in each direction.

It should also be noted that in the future it would be reasonable to use several stars in a region to estimate the beam transmittance for that region. It would also be reasonable to add a feature which compares the signal from the star with the background signal, and makes an automatic assessment of whether the star signal is bright enough to be useful.

5.0 System Calibration

The WSI was returned to MPL for calibration on 21 March 01. It was then sent to Photometrics for routine maintenance. It turned out to be necessary to return it to Photometrics again for replacement of a bad receiver card. We also replaced the shutter, and checked the filters for aging. The system was calibrated in April and May 01, and returned to the sponsor 29 May 01.

The system was calibrated using a 3 meter optical bench, and a FEL1000 lamp traceable to NIST. Effective lamp irradiances in the WSI spectral filters were determined from the measured lamp spectral irradiance, filter spectral transmittances, and sensor spectral sensitivity. The calibrations included the following:

Linearity and Exposure Calibrations
Absolute Radiance in each filter combination
Aperture Calibration
Flat Field
Rolloff
Geometric Calibration

The calibrations are fully documented in in-house memoranda.

A program ImgCal was written in C, to process field images to yield fully calibrated radiance distributions. This program is also documented in an in-house memo. This program was used to process field data to produce the radiance images used for testing the transmittance techniques.

A technique was developed by one of our sponsors for a higher precision geometric calibration. With their permission, we modified this technique for easier application. Our Air Force sponsors for the current project needed to extract the higher precision calibration for Unit 5, so these programs and the tutorial were delivered to our sponsors. The technique is not trivial, and further upgrades were developed and delivered.

The actual data for Unit 5 was not accessable to us due to security issues, so the remainder of the analysis was done using data from the Air Force's SOR site. This SOR data was acquired with one of our WSI units.

6. Inherent Star Irradiance Library

As discussed in Section 4, the first step in the determination of the beam transmittance mapping with the WSI is determination of the inherent irradiance library. As discussed in Section 4, there are several areas of potential error that may contribute to incorrect values of inherent irradiance. Some of the error sources listed there include the definition of a zero-magnitude source for visual magnitudes, the location of the peak in the visual response curve, and a star's color temperature, which is estimated based on its spectral class. The values of the first two variables are discussed in that memo, while the spectral class – color temperature correspondence deserves further mentioning.

Each star is assigned a spectral class and subclass based on its spectra, which corresponds to a specific star color temperature. For this study, a spectral class table with 133 classifications from the Jet Propulsion Lab was used: http://spider.ipac.caltech.edu/staff/gerard/q_refs/sptype_temp.html. Because the spectral classes and subclasses actually include a range of temperatures, a given star's spectral class represents only an estimate of the actual color temperature. The varying color temperatures assigned to specific stars by different sources can lead to inherent radiances that differ by as much as 10% or more. For example, two sky map software packages list Aldebaran as 3406 K and 4320 K, which leads to a calculated inherent irradiance of 1.67E-8 and 1.85E-8 W/m^2-μm, respectively (assuming the same star magnitude). Aldebaran has been assigned a spectral class of K5, which, according to the spectral class table used here has a corresponding color temperature of 3920 K.

Equation 13 was used to obtain the inherent spectral irradiance for each star. The constant, C, in that equation was calculated in each case using Equation 14. The visual response curve given in Table 1 was used for the integral in the bottom half of that equation. Effective blackbody emittances were calculated using a modified version of the in-house software Program Filter. To system response for this instrument were also correct to the standard WSI response, as documented in in-house memos. Figure 1 shows the resulting inherent spectral irradiances calculated with this method as a function of visual magnitude for all stars in the NASA star library.

7. Apparent Star Irradiance and Transmittance

While the inherent irradiance for a star need only be calculated a single time and stored for later retrieval, the apparent irradiance is determined for stars during image processing. In order to conduct the transmittance study, WSI imagery had to be radiometrically calibrated. As noted in Section 5, software called ImgCal was written that calibrates either a single image or a directory of images. Imgcal was used to calibrate several days of WSI imagery used in the transmittance project.

The latest version of the nighttime cloud algorithm, called StarCloudAlg1, was used to identify stars in each nighttime WSI image. The software is documented in in-house memo AV03-030t. The NASA star catalog used in the software had to be modified to include inherent spectral irradiances, which are described in Section 6. The night

algorithm software had to be modified to calculate and output measured spectral irradiance and transmittance for identified stars.

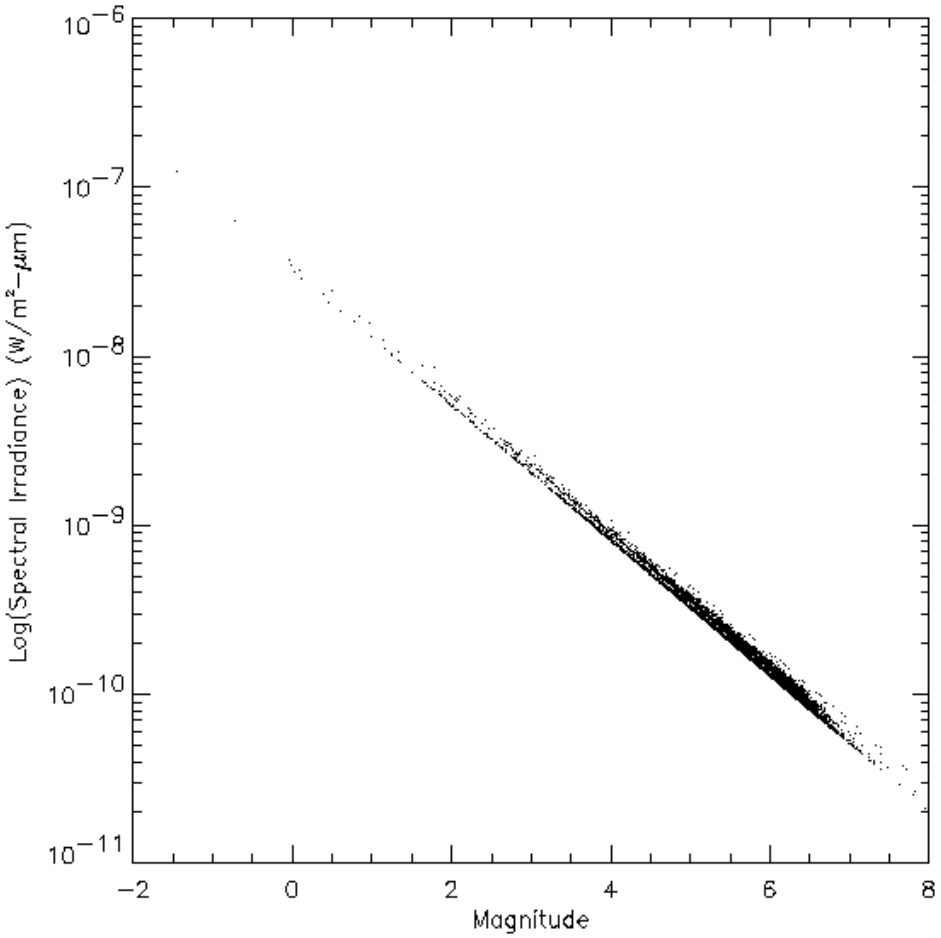

Figure 1. Calculated inherent spectral irradiances for stars found in the NSSDC Bright Star Catalog.

To convert image pixel values to star flux, it was decided that for the initial study, simply adding pixels surrounding the predicted star location and correcting for the sky background would suffice. The alternative method would be to integrate a best-fit Gaussian curve placed at the star center. Anecdotal evidence suggests that the Gaussian method works better, particularly in a crowded star field. Initial tests showed that the results were similar when examining large datasets. We were concerned about pixellation effects described below, so we decided to use the pixel addition method for this study. This issue is one that could be examined further in the future.

One aspect of the determination of star energy from the Gaussian method that has not been adequately addressed for this study is the pixellation effect mentioned in Memo AV01-097t. Basically, if the star is centered on a pixel, we believe the best-fit procedure used to locate stars handles the central pixel value as though it is equal to the star peak value, rather than the star signal integrated over the area of the pixel. Methods were

developed to correct for this, however they did not improve the results. Therefore no pixellation correction was used for this study.

The current method of calculating apparent star irradiance involves summing a 5 X 5 pixel array of signals surrounding the star center pixel. The signals are modified by subtracting the background value (as determined by the Gaussian best-fit) and multiplying by the solid angle for the pixel. The resulting sum equals the apparent star irradiance.

As shown in Equation 24, transmittance in an isotropic atmosphere should drop off toward the horizon. In the current version of the night algorithm containing these irradiance calculations, the irradiances can be corrected for these atmospheric extinction effects using T(0) = 0.70 in order to estimate the cloud transmittance without the aerosol effects. The correction can easily be removed or modified by using the following multiplicative factor:

$$E_m = E_0 \left(\frac{0.70}{T_m} \right)^{\sec\theta} \qquad \text{EQ (25)}$$

where T_m is the modified cloud-free transmittance, E_0 is the irradiance computed using T(0) = .7, and E_m is the modified irradiance.

Estimated atmospheric transmittance at the location of a star may be calculated by dividing the measured value of spectral irradiance by the inherent spectral irradiance found in the star catalog. By combining the transmittance results over an image, a transmittance map can be obtained.

8. Results

Results presented here were derived using cloud-free SOR imagery from February 14, 1999. In Figure 2, inherent and measured spectral irradiances are compared using catalog stars up to magnitude 6 and star zenith angles < 60°, for a total of 32,714 stars. These initial results clearly show a reasonable correlation (0.84) between inherent and measured irradiances. The red line in the plot represents a simple best fit line. As Figure 1 shows, higher spectral irradiances correspond with lower visual magnitudes, although the relationship is not direct, as previously stated. Lower irradiances show significantly higher variability than higher irradiances due to difficulties associated with determining the measured (and inherent) irradiances for faint stars. Figure 3 shows similar data for some of the brighter stars (spectral irradiances greater than 10^{-9} W/m^2-μm, for a total of 1555 stars). The correlation for these stars is much higher, 0.99, as expected.

It should be noted that although these were the results at the time of the completion of the project, the transmittance work has been continued under funding from another sponsor. This work resulted in a significant improvement in the correlations, from 0.84 correlation to 0.96 correlation. We are continuing evaluating sources of uncertainties at the time of this writing, however this work is not included in this contract report.

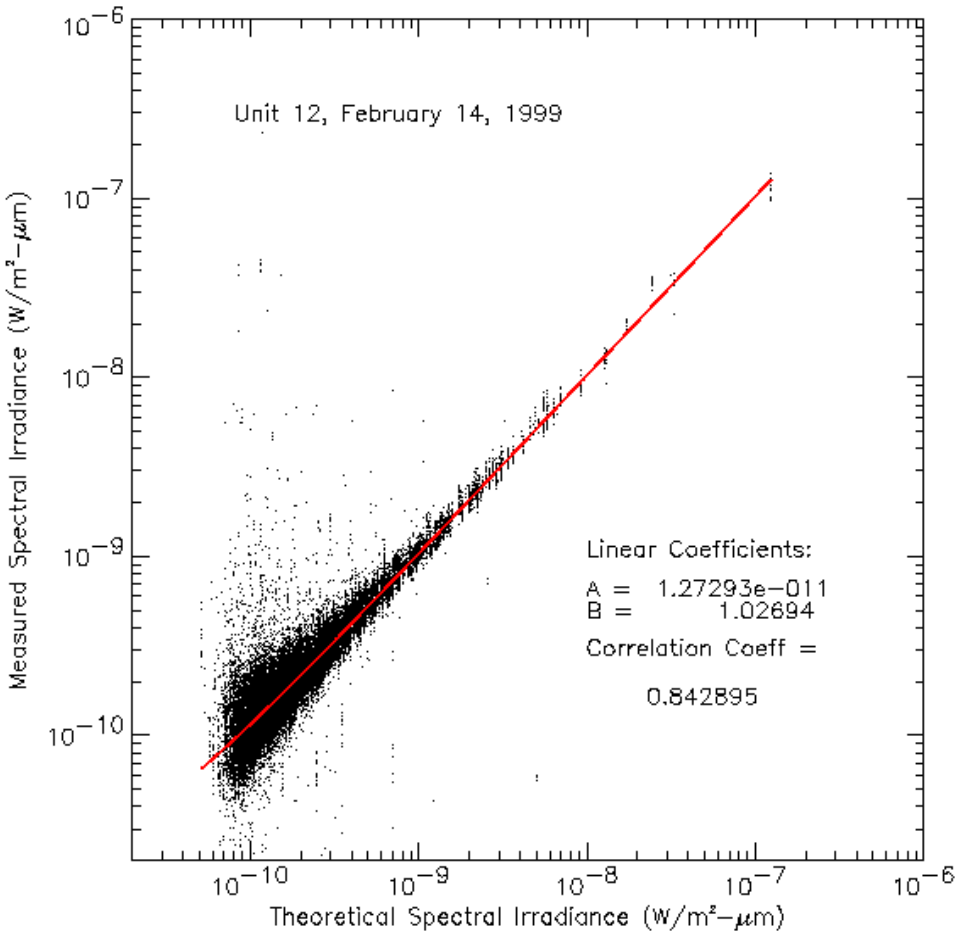

Figure 2. Spectral irradiances for WSI passband. Stars to Magnitude 6. Zenith angles < 60°. Red line is linear best fit of data.

Results were also extracted for individual stars. Figure 4 shows how the transmittance changes for a specific star as a function of zenith angle, as well as a function of changes in T(0). We expect the transmittance to vary less when using the best estimate of T(0). For this example, a vertical earth-to-space transmittance of 0.90 yields the most consistent (flat) curve as a function of zenith angle. In most of the cases we examined, T(0) = 0.8 yielded the most consistent transmittance results for zenith angles < 60°. Although 0.7 is a nominal earth-to-space vertical beam transmittance for the photopic, we would expect it to be closer to 1 for the WSI open hole configuration, which corresponds most closely to a red filter.

Note that the curve for T(0) = 0.9 does not intersect the y axis at 0.9. This most probably indicates a calibration offset. From multiple plots such as shown in Fig 4, we estimated the calibration correction to be a factor of 0.89. This corresponds closely with a calibration correction due to pixel cross-talk that we recently measured.

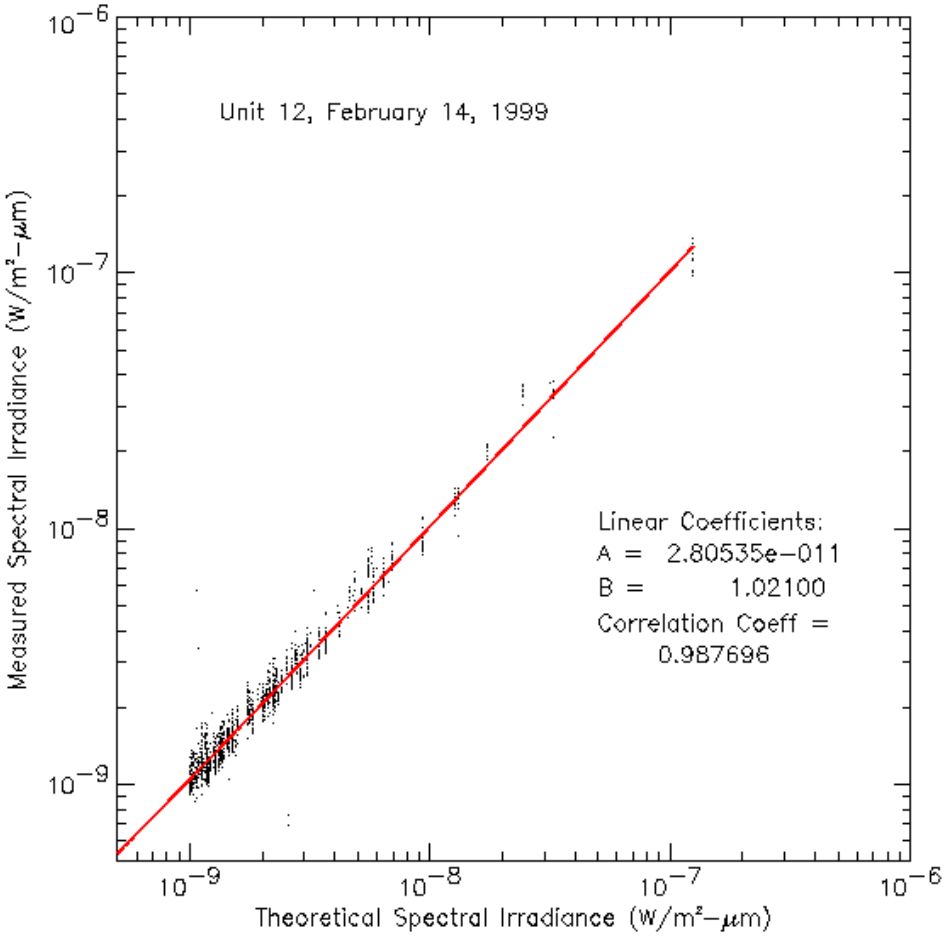

Figure 3. Spectral irradiances for WSI passband. Stars with spectral irradiances greater than 10^{-9} W/m^2-μm. Zenith angles < 60°. Red line is linear best fit of data.

Another possible source of error is the estimate of inherent irradiance. The zenith angle dependence indicates that there may be stray light or rolloff issues to consider. The variance in measured irradiance for a given star demonstrated here is also seen in Figures 2 and 3, where the measured irradiances for a given star line up along a line at constant theoretical irradiance. Some of this variance in the corrected measured irradiances may have to do with the aerosol correction, and some may be due to uncertainties in the extraction of the measured irradiance.

Figures 5-10 show several preliminary transmittance maps that demonstrate the potential of the technique using calibrated imagery from SOR. Each star in the dataset is identified by a box with a color representative of the calculated transmittance. The key for the colors is shown on each page. Only stars that were magnitude 6 or less were used. Additionally, stars in a crowded field were eliminated. For all cases, a correction factor was applied that accounts for an error in the calibration constant for Unit 12. The first four cases present total transmittance, while the last two cases present cloud transmittance including a correction for estimated aerosol transmittance (T(0) = 0.8).

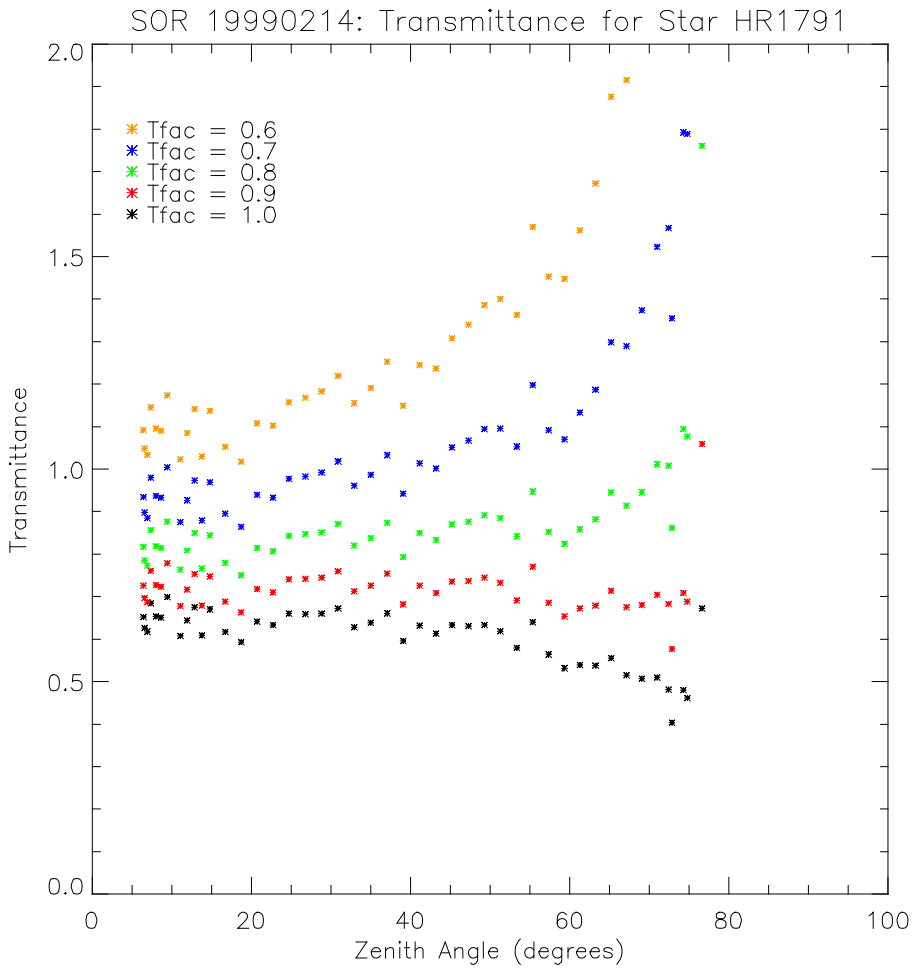

Figure 4. Transmittance for star HR1791 using various values of T(0). Results were compiled from multiple images.

Figure 5 is a cloud-free image that was used to create the composite dataset used in Figures 2 and 3. Because this plot is not corrected for aerosol transmittance, we would expect the transmittances to be somewhat less than 1 and to drop off toward the horizon. The transmittances at lower zenith angles (e.g. overhead) are mostly in the range 0.4-1.0. There is clearly more variance than we would like, however the results appear to be in the right ballpark. Where stray light from Albuquerque to the northwest exists, many stars were not found (red squares). While the range of values is wide in this image, as thin cloud moves into the field of view, it is apparent that the cloud-free portions of an image can be distinguished, as demonstrated in the next three figures.

Figure 6 is a case with wispy thin cloud moving into most of the frame with somewhat thicker cloud to the south. The difference in transmittance is seen throughout the image, as green is predominant color (0.4-0.6) rather than the purple (0.6-0.8) from the previous clear image. There are also many more yellow (0.2-0.4) and red (no star) cases here. In cases with more cloud, as shown in Figure 7, transmittances drop even more. Figure 8 is

a nice example that includes a large semi-opaque cloud band that crosses the image. To the southeast and northwest, where the sky is mostly clear, the pattern of colors resembles that of Figure 5.

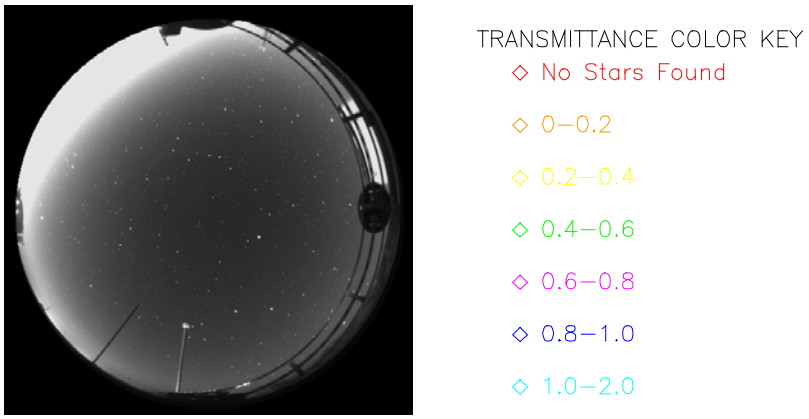

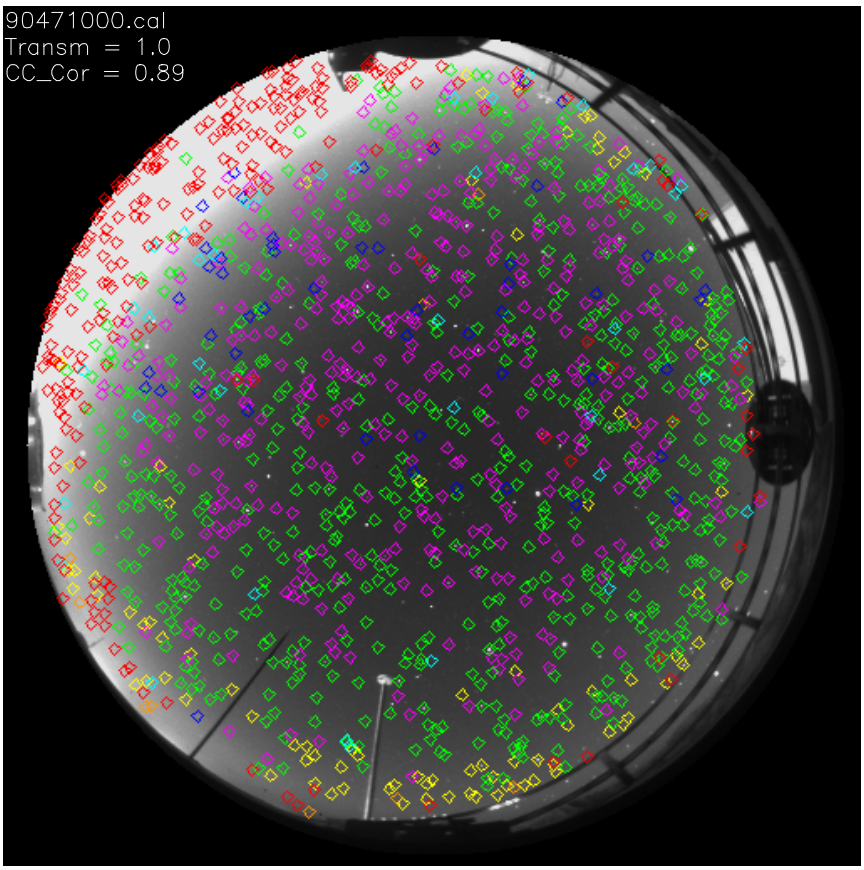

Figure 5. Transmittance map for cloud-free image. No aerosol correction applied. Calibration correction of 0.89 applied.

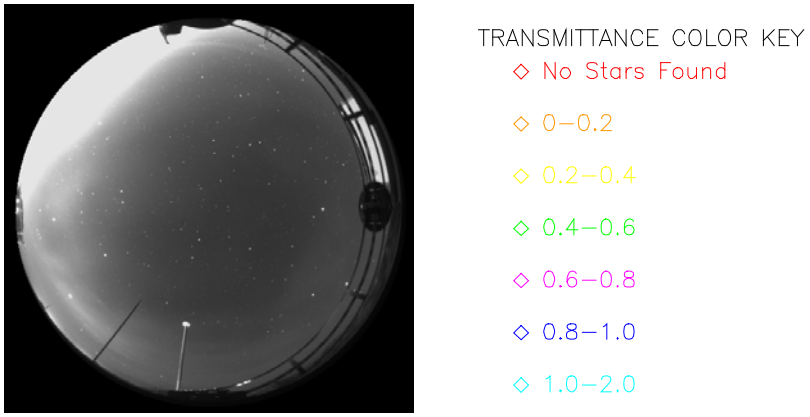

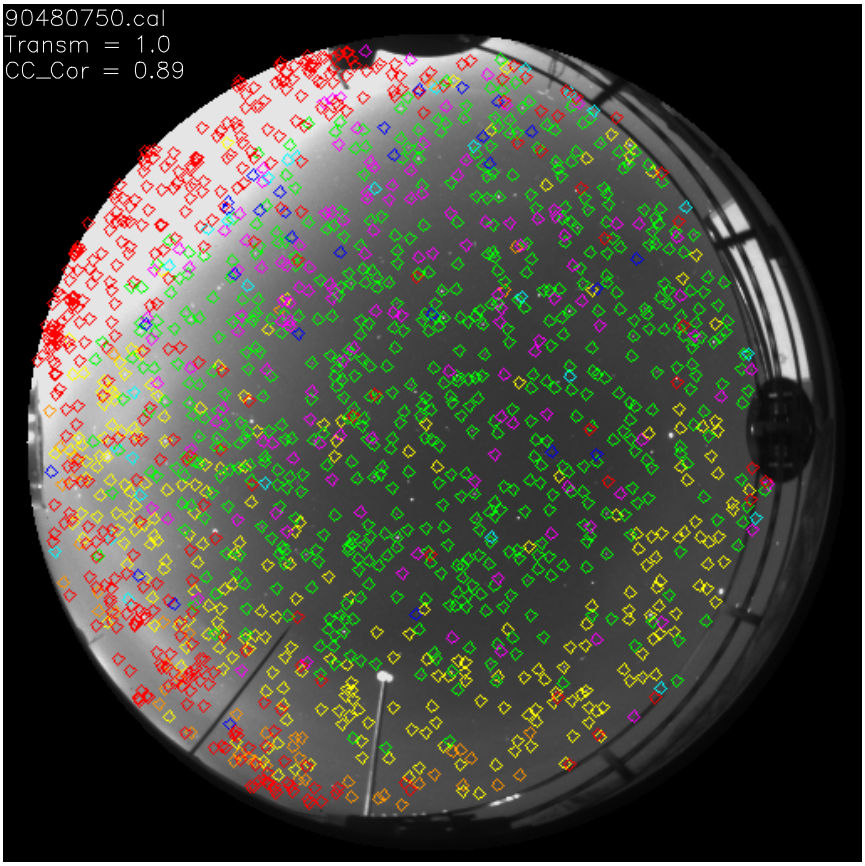

Figure 6. Transmittance map for thin cloud image. No aerosol correction applied. Calibration correction of 0.89 applied.

A couple of cases were also included that have an estimate of an aerosol transmittance correction applied. This accounts for the reduction of clear sky transmittance toward the horizon. Figure 9 is an aerosol-corrected cloud-free case, also used in Figure 5. The transmittances here are higher, and the drop-off in transmittance at the horizon is no longer apparent. Figure 10 shows similar results for the partly cloudy case also shown in Figure 8.

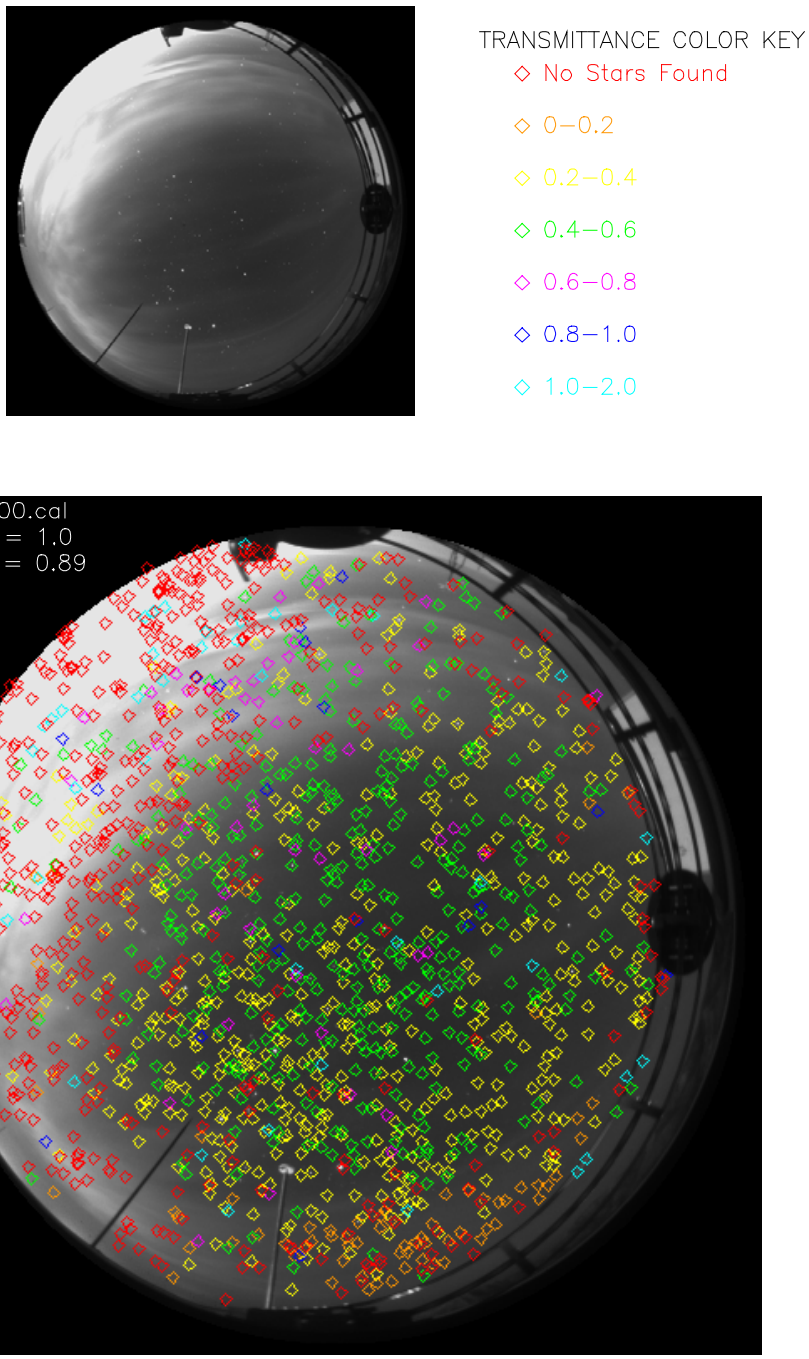

Figure 7. Transmittance map for another thin cloud image. No aerosol correction applied. Calibration correction of 0.89 applied

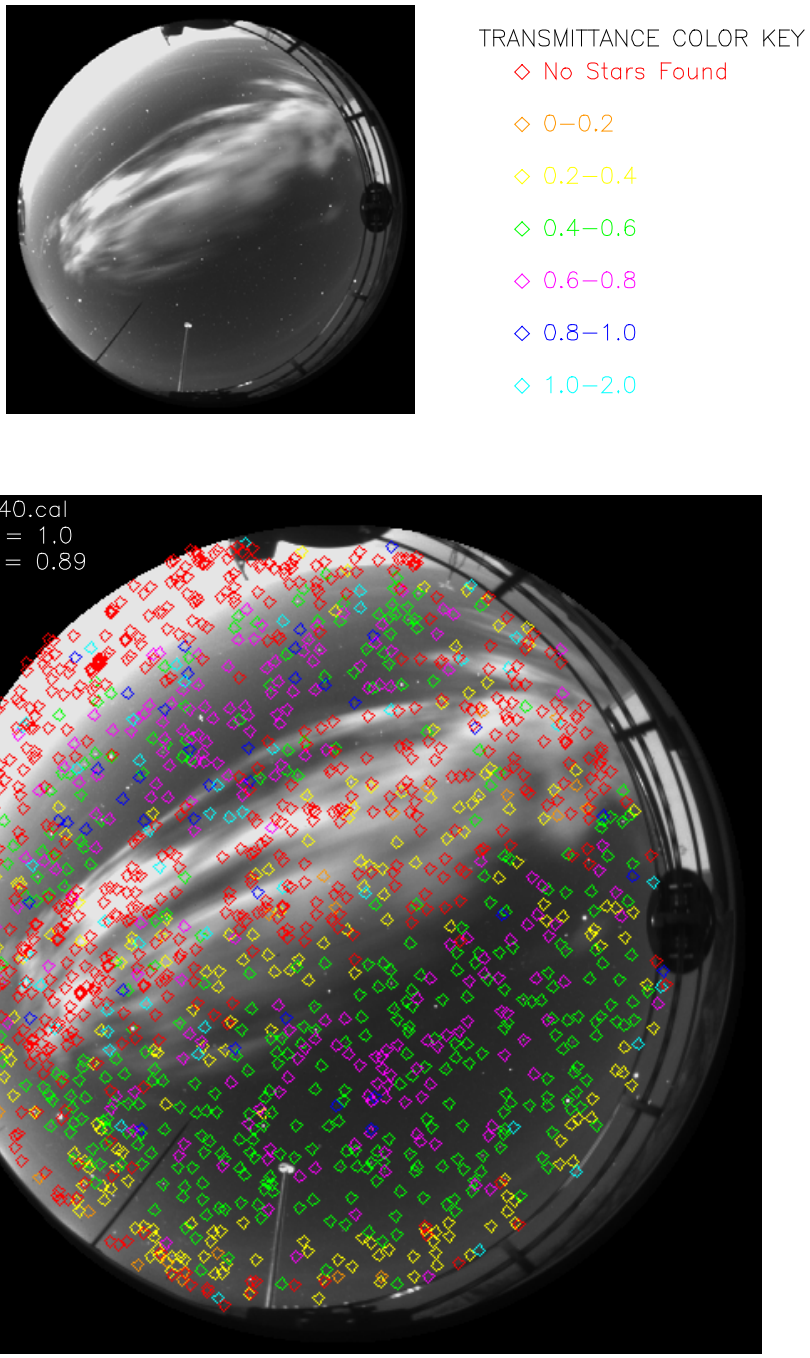

Figure 8. Transmittance map for partly cloudy image. No aerosol correction applied. Calibration correction of 0.89 applied.

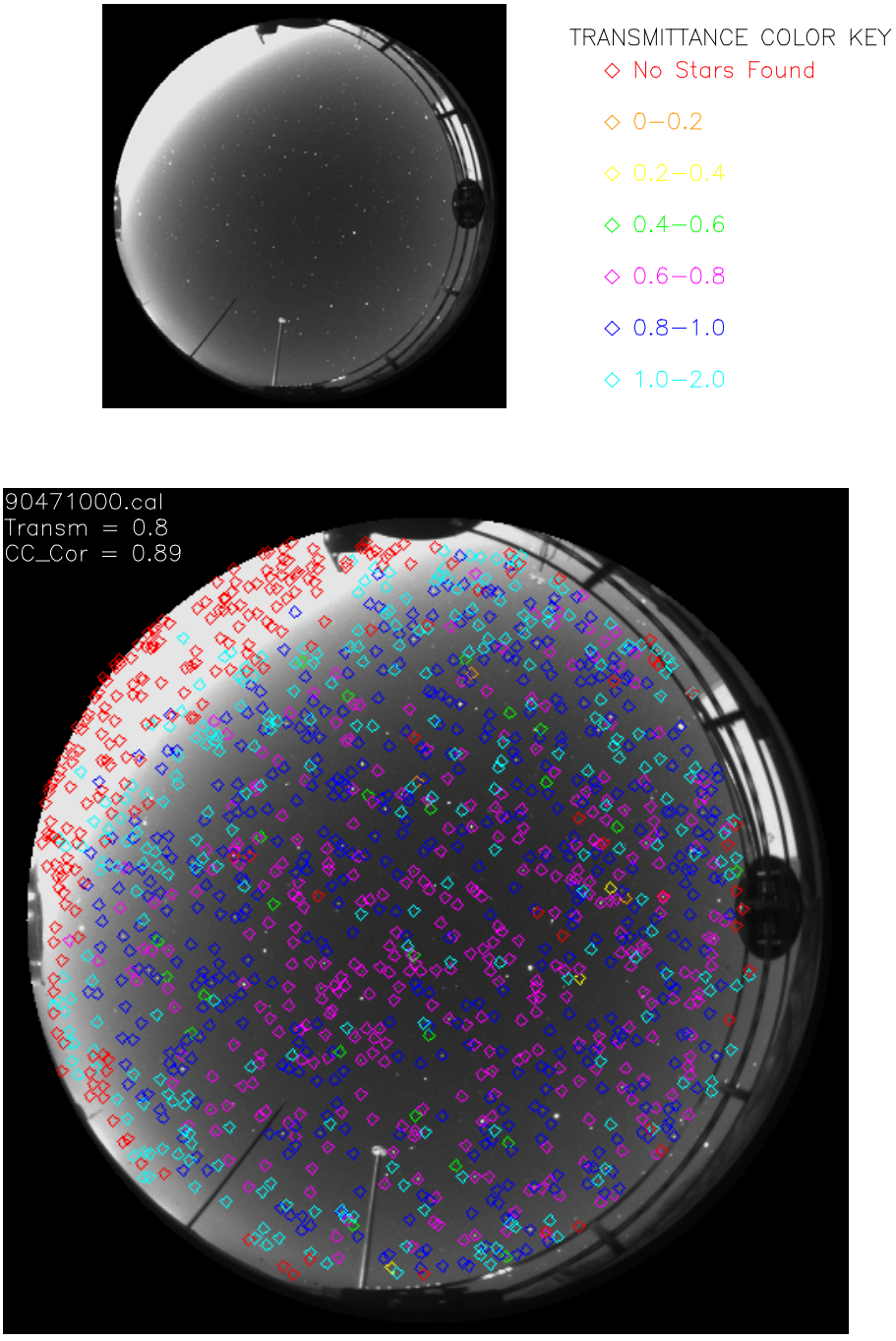

Figure 9. Transmittance map for cloud-free image (same image as Fig 5). 0.8 aerosol correction applied. Calibration correction

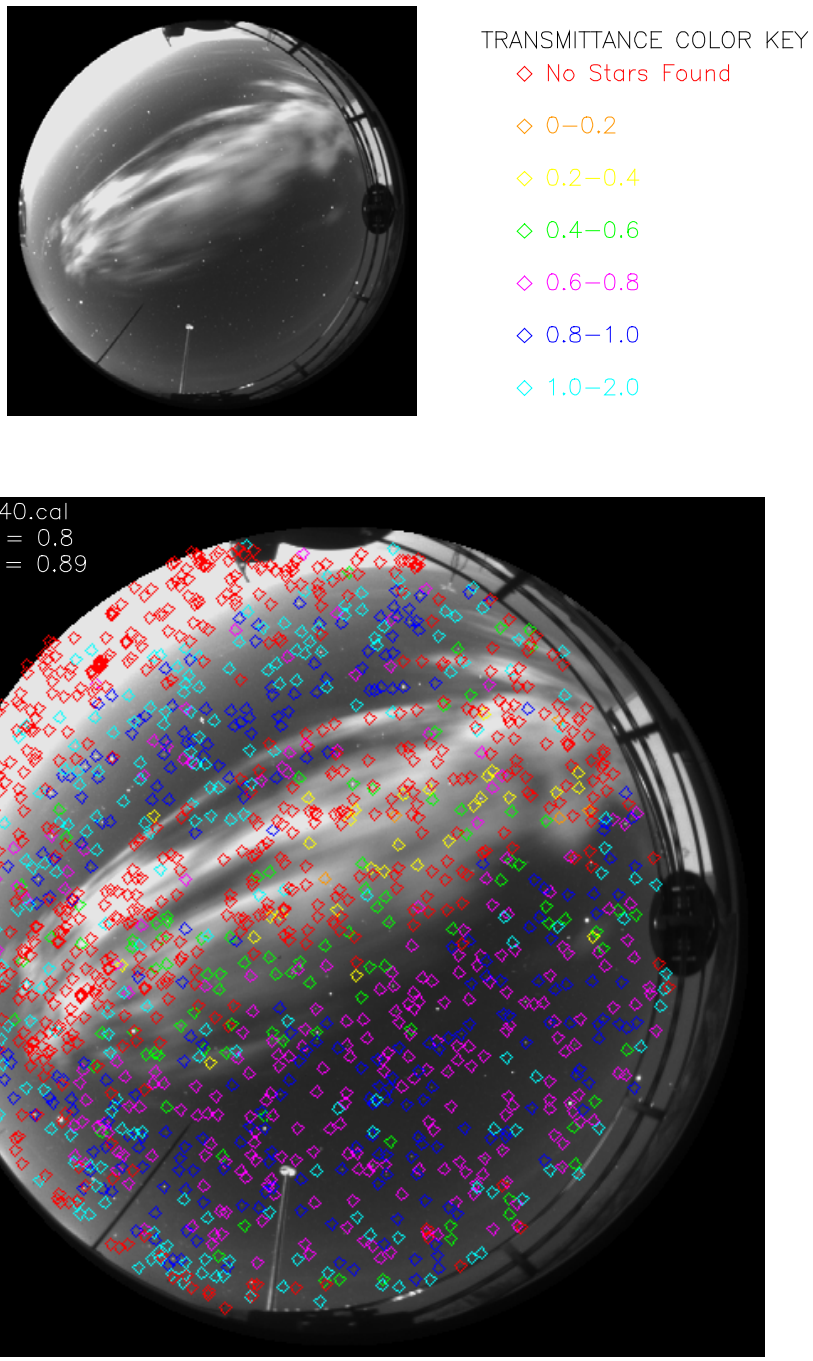

Figure 10. Transmittance map for thin cloud image (same image as Fig. 8). 0.8 aerosol correction applied. Calibration correction of 0.89 applied.

9. Discussion of Transmittance Results

With some reasonable results in hand that demonstrate that the instrument calibration and the approach documented in Section 4 are both on target, we can now look toward how errors in the results can be reduced. One observation that jumps out is the large variance found in the measured irradiances for a given star under cloud-free conditions. It would be a good idea to pick a few stars and take a closer look at why the variation occurs. One possibility is to address the pixellation effect mentioned earlier, which is likely to be a significant source of variance in the results. We may also be able to correct errors in the calculated inherent spectral irradiances that were added to the star catalog by examining results for individual stars over a number of days. The use of calibration stars for determining the current vertical earth-to-space aerosol transmittance and generally checking the calibration is another potentially fruitful approach. In general, we are very pleased with these initial results, and feel that this technique has significant potential for determining beam transmittance distribution over the sky dome.

10. Summary

Under this contract, we were primarily tasked to develop a library of inherent star irradiances, calibrate the sensors to provide the absolute radiance field, evaluate techniques for determining earth-to-space beam transmittance distribution from WSI starlight imagery, and, within the limits of funding, work toward development of these techniques in software code which can be fielded with the AFRL WSI. This work was successfully completed.

The equations for extracting transmittance from WSI data were developed, and then tested. The results were converted to a stand-alone program written in C, that produces maps of transmittance over the full sky. While the results are not yet as precise as we would like, we are pleased with the results. Work on these techniques is presently continuing under funding from another sponsor.

11. Acknowledgements

We would like to express our appreciation to Capt. Dan Gisselquist, and Capt. Craig Phillips of Air Force Research Labs, Kirtland Air Force Base, for their work with us on this project. We would also like to thank Clint Campbell and Wil Gravemen of Logicon, who were also working on our sponsor's project, and were a pleasure to work with. Finally, thanks to Starfire Optical Range for the use of the data.

12. References

Allen, C.W., (1976), "Astrophysical Quantities", The Athlone Press, London and Dover, New Hampshire.

Budding, E., (1993), "An Introduction to Astronomical Photometry", Cambridge University Press.

Boyd, R. W., (1983), “Radiometry and the Detection of Optical Radiation”, John Wiley & Sons, New York, Wiley Series in Pure and Applied Optics.

Duntley, S. Q., R. W. Johnson, and J. I. Gordon (1975), “Airborne Measurements of Optical Atmospheric Properties in Western Washington” University of California, San Diego, Scripps Institution of Oceanography, Visibility Laboratory, SIO Ref. 75-24, AFCRL-75-0414.

Johnson, R. W., W. S. Hering and J. E. Shields (1989), “Automated Visibility and Cloud Cover Measurements with a Solid-State Imaging System”, Marine Physical Laboratory, Scripps Institution of Oceanography, University of California San Diego, SIO 89-7, GL-TR-89-0061, NTIS No. ADA216906

Johnson, R. W., J. E. Shields, and T. L. Koehoer (1991), “Analysis and Interpretation of Simultaneous Multi-Station Shole Sky Imagery”, Marine Physical Laboratory, Scripps Institution of Oceanography, University of California San Diego, SIO 91-3, PL-TR-91-2214

Lena, P. (1988), “Observational Astrophysics”, Springer-Verlag, Berlin/Heidelberg, Germany.

McCartney, E. J. (1976), “Optics of the Atmosphere”, John Wiley & Sons, New York, Wiley Series in Pure and Applied Optics.

Ramsey, R.C. (1962), “Spectral Irradiance from Stars and Planets, above the atmosphere, from 0.1 to 100.0 Microns”, Applied Optics, Vol. 1, No. 4, July, 1962.

Riker, J., (1997), “TEM 97-135: Addition of a magnitude-temperature (m_v-T) script to ARC version 16.1”, in-house memorandum from Air Force Research Lab at Kirtland Air Force Base

Riker, J.F., (1993), “TEM 93-40: Absolute Radiometry”, in-house memorandum from Air Force Research Lab at Kirtland Air Force Base

Shields, J. E., R. W. Johnson, and T. L. Koehler, (1993), “Automated Whole Sky Imaging Systems for Cloud Field Assessment”, Fourth Symposium on Global Change Studies, 17 – 22 January 1993, American Meteorological Society, Boston, MA

Shields, J. E., R. W. Johnson, M. E. Karr, R. A. Weymouth, and D. S. Sauer, (1997a), “Delivery and Development of a Day/Night Whole Sky Imager with Enhanced Angular Alignment for Full 24 Hour Cloud Distribution Assessment”, Marine Physical Laboratory, Scripps Institution of Oceanography, University of California San Diego, Report MPL-U-8/97

Shields, J. E., M. E. Karr, and R. W. Johnson, (1997b), “Service Support for the Phillips Laboratory Whole Sky Imager”, Marine Physical Laboratory, Scripps Institution of Oceanography, University of California San Diego, Report MPL-U-10/97

Shields, J. E., R. W. Johnson, M. E. Karr, and J. L. Wertz, (1998), “Automated Day/Night Whole Sky Imagers for Filed Assessment of Cloud Cover Distributions and Radiance Distributions”, Tenth Symposium on Meteorological Observations and Instrumentation, 11 – 16 January 1998, American Meteorological Society, Boston, MA

Shields, J. E., M. E. Karr, A.R. Burden, R.W. Johnson, and J. G. Baker, (2002), “Analytic Support for the Phillips Laboratory Whole Sky Imager, 1997 - 2001”, Marine Physical Laboratory, Scripps Institution of Oceanography, University of California San Diego.

Zombeck, M.V. (1990), “Handbook of Space Astronomy and Astrophysics”, Cambridge University Press, Cambridge, England.